ORIGINAL PAPER

GluN2A/B ratio elevation induced by cortical spreading depression: electrophysiological and quantitative studies of the hippocampus

Panupong Hansrivijit · Suteera Vibulyaseck · Montree Maneepark · Anan Srikiatkhachorn · Saknan Bongsebandhu-phubhakdi

Abstract Cortical spreading depression (CSD), an underlying mechanism of migraine aura, propagates to the hippocampus, and might explain hippocampus-associated symptoms during migraine attack. We hypothesised that this process is, some parts, mediated by NMDA receptors. By using a rat model, CSD was elicited by solid KCl for 45 minutes prior to electrophysiological and quantitative analyses. The result from electrophysiological study was the ratio of glutamate NMDA receptor 2A and 2B subunits (GluN2A/B). Total NMDA receptor response was isolated using an AMPA antagonist, prior to a GluN2B receptor antagonist. The GluN2A/B ratio was calculated by dividing the remaining NMDA-mediated field-excitatory synaptic potentials (fEPSP) with the subtracted difference of NMDA-mediated fEPSP. Western blot analysis of the hippocampus was performed to confirm the quantitative change of GluN2A/B ratio. In hippocampal slice study ($n = 12$), the GluN2A/B ratio of hippocampal fEPSP was significantly increased in CSD group. Western blot analysis ($n = 30$) revealed an increase in GluN2A subunits and a decrease in GluN2B subunits in the hippocampus ipsilateral to the CSD induction. Our current study revealed that GluN2A/B ratio was shown to be elevated following CSD stimulation by increasing the total number of GluN2A while reducing the total number of GluN2B subunits. This ratio was demonstrated to be associated with synaptic plasticity of the hippocampus in numerous studies. In conclusion, we showed that CSD increased GluN2A/B ratio, in turn, would result in altered synaptic plasticity. Our findings provide a probable implication on the correlation of migraine aura and hippocampus-associated symptoms.

Keywords NMDA receptors · migraine aura · transient global amnesia (TGA) · hippocampal spreading depression · long-term potentiation (LTP) · AMPA receptors

P. Hansrivijit · S. Vibulyaseck · M. Maneepark ·
A. Srikiatkhachorn · S. Bongsebandhu-phubhakdi (✉)
Department of Physiology, Faculty of Medicine, Chulalongkorn University, Bangkok, Thailand
e-mail: saknan@live.jp

S. Vibulyaseck
Medical Research Institute, Tokyo Medical and Dental University, Tokyo, Japan

M. Maneepark
Department of Biology, Faculty of Science, Srinakharinwirot University, Bangkok, Thailand

Introduction

Various cerebral insults (e.g. epileptic crises, trauma, ischemia, haemorrhage, and migraine) were shown to produce a transient disturbance in cortical activity, so-called cortical spreading depression (CSD). Cortical spreading depression is caused by massive redistribution of ions, particularly potassium and hydrogen ions between intracellular and extracellular compartments [1] resulting in cortical depolarisation that can spread to the adjacent areas. By adopting a model of migraine with aura, spreading depression (SD) in each cortical area is accountable for different clinical manifestations seen in the patients. For instance, CSD in the occipital cortex can cause visual metamorphopsia [2, 3], whereas those occur in the somatosensory cortex result in paraesthesia or hemi-anaesthesia [4].

Spreading depression propagated to the hippocampus is believed to cause amnesia, emotional and behavioural changes (e.g. hyperactivity, yawning) during migraine attack [5]. In case of acute amnesia, it seems to be transient (4-8 hours in duration) and may impair both anterograde and retrograde memory. Long-term association of migraine and amnesia was also demonstrated in a retrospective cohort study suggesting that migraine is a risk factor of developing transient

global amnesia (TGA) [6]. For decades, Olesan and Jorgensen proposed that the association between migraine and TGA may be explained by presence of spreading depression in the hippocampus [7]. The hypothesis was later proven by groups of *ex vivo* and *in vitro* experiments showing that CSD propagated to the hippocampus. Limited studies were published regarding the presence of SD in the *in vivo* hippocampus following CSD except in familial hemiplegic migraine type 1 (FHM1) mutant mice [8]. Although the molecular mechanisms underlying the correlation of migraine and TGA are still unclear, existing evidence suggested that the process may involve actions of glutamatergic receptors [9].

Glutamatergic transmission is known to play an important role in inducing plastic change in the hippocampal synapse. Repetitive activation of the hippocampal synapse can result in a long-lasting change in synaptic activity known as long-term potentiation (LTP). This process is an important step in the registration and consolidation of new memories. Various classes of glutamatergic receptors are involved in LTP development, specifically α-amino-3-hydroxy-5-methyl-4-isoxazolepropionic acid (AMPA) and *N*-methyl-D-aspartic acid (NMDA) receptors. Previously, our group showed that CSD significantly reduced LTP magnitude by decreasing post-synaptic AMPA receptor response [9]. However, the effect of CSD on hippocampal NMDA receptor activity were not demonstrated. Differential subunits of NMDA receptors mainly detected in the hippocampus are GluN2A and GluN2B subunits [10]. Thus, these receptors are of our particular interest. Additional studies have demonstrated that GluN2A/B response ratio is strongly associated with synaptic plasticity by modifying LTP induction threshold [11-13].

In this study, we aimed to demonstrate the changes in synaptic transmission of NMDA receptors. We identified existence of SD observed in the rat hippocampus and compared their differences in electrical properties with the original CSD. Sequential changes in NMDA receptor activity were reported in terms of GluN2A/B response ratio. Quantitative assays of GluN2A and GluN2B subunits were also performed using Western blot analysis. The findings of this study may imply a clinical correlation between migraine and hippocampus-associated symptoms.

Methods

Animals

Adult male Wistar rats (National Laboratory Animal Centre, Mahidol University, Nakorn-Pathom, Thailand) weighing 200-350 g were recruited in this study ($n = 50$).

The animals were acclimatised to the housing facility for at least seven days prior to the experiments. The study was conducted according to the guideline for experimental animals suggested by the National Research Council of Thailand. The study protocol was approved by the Ethics Committee of the Faculty of Medicine, Chulalongkorn University (No.012/2553).

Animal preparations

Each rat was anaesthetised with 60 mg/kg of sodium pentobarbital (Ceva Sante Animale, Libourne, France) intraperitoneally. We avoided using inhaled isoflurane or IV dexmedetomidine as surgical anaesthetics due to their effects on suppressing CSD frequency [14]. Physiological parameters were monitored and only animals that were in stable condition throughout the preparation were included in the experiment. All anatomical landmarks guided by Paxinos & Watson's brain atlas [15].

CSD induction

The rat's head was fitted to a stereotaxic apparatus (Narishige, Tokyo, Japan). After the right parietal bone had been exposed, a 2-mm craniotomy was performed at 6 mm posterior to the bregma and 2 mm lateral to the sagittal suture using an electric dental driller (NSK, Tokyo, Japan). Since propagation of CSD into the hippocampus usually occurred under hyper-excitable conditions, induced either pharmacologically or genetically, increased dose of KCl was employed in our study. For CSD induction, 3 mg of solid KCl (Sigma-Aldrich, St. Louis, MO, USA) was topically applied onto the dura mater for 45 minutes. In control rats, 3 mg of solid NaCl (Merck, Darmstadt, Germany) was used instead of solid KCl.

In vivo cortical DC recording

For the DC recording ($n = 4$), a 2-mm diameter craniotomy was performed in the right frontal bone (from bregma: anterior-posterior, +3 mm; lateral, 2 mm; and dorsal-ventral, 0.5 mm). A recording glass microelectrode for detecting the DC potential was inserted into the frontal neocortex to a depth of 500 μm. Analogue data were converted into digital format using. The data were then analysed using MP100 (Biopac Systems Inc., Goleta, CA, USA) and AcqKnowledge acquisition software (Biopac Systems Inc., Goleta, CA, USA). The measured variables included the area under the curve (AUC) and the amplitude of each CSD wave as well as the number of CSD waves that occurred within a 45-minute period.

In vivo hippocampal DC recording

In a separated set of experiments (n = 4), the DC potential was recorded in the CA1 region of the hippocampus instead of the neocortex (from bregma: anterior-posterior, -4 mm; lateral, 2 mm). A recording glass microelectrode was inserted with a depth of 2.2 mm with the aid of rat brain atlas [15] and previous electrophysiological study [16]. The histological position of the electrode was confirmed microscopically.

Hippocampal slice preparation

After 45 minutes of CSD stimulation using solid KCl, the animals (n = 6, each group) were decapitated and their ipsilateral hippocampal tissues were entirely dissected. These tissues were then quickly loaded and sectioned using a Vibratome tissue slicer (Vibratome, Richmond, IL, USA). The tissues were processed in cooled artificial CSF solution (119 mM NaCl, 26.2 mM NaHCO$_3$, 11 mM glucose, 2.5 mM KCl, 2.5 mM CaCl$_2$, 1.3 mM MgSO$_4$, 1.0 mM NaH$_2$PO$_4$, 0.1 mM picrotoxin; a GABA$_A$ receptor antagonist), bubbled with carbogen (95 % O$_2$, 5 % CO$_2$). Fresh slices were moved to a humidified interface-type holding chamber and recovered for at least 1.5 hours prior to the performance of the electrophysiological study.

Electrophysiological recording

A continuation between the CA1 and CA3 region was terminated in order to prevent epileptiform activity originating from the CA3 region. A bipolar tungsten-stimulating electrode was placed in the Schaffer collaterals to evoke a postsynaptic response by delivering a square-pulse stimulus at 0.1 Hz for 0.2 msec. Discharges from presynaptic fibres followed by fEPSPs were recorded using a glass microelectrode. Only slices that produced fEPSP amplitudes of more than 1 mV and were stable for at least 15 minutes were included in this study.

Response ratio of GluN2A/B

After stable baseline fEPSPs were recorded for at least 15 minutes, NMDA receptor-mediated fEPSPs were isolated by bath application of a potent AMPA receptor antagonist, 6-cyano-7-nitroquinoxaline-2,3-dione; CNQX (10 µM in 0.1 % DMSO; Tocris Bioscience, Bristol, UK) to exclude signals from AMPA components. Ten minutes after application of the drug, input stimulation was delivered at 0.033 Hz and its intensity was adjusted to evoke stable NMDA receptor-mediated fEPSPs. Ten minutes later, the GluN2A component of NMDA receptor-mediated fEPSPs was isolated by bath

application of CNQX (10 µM) and GluN2B subunit-selective NMDA receptor antagonist, ifenprodil (3 µM in 0.1 % DMSO; Tocris Bioscience, Bristol, UK) for 1 hour.

Total component of NMDA receptor responses was the averaged AUC of the NMDA receptor-mediated fEPSPs during 10 minutes prior to ifenprodil application. The amplitude of NMDA receptor-mediated fEPSPs was normalised in the range of 0.5-1.5 mV. GluN2A component of NMDA receptor responses was the averaged AUC of the NMDA receptor-mediated fEPSPs during 50-60 minutes after ifenprodil application (i.e., ifenprodil-insensitive component). GluN2B component (i.e., ifenprodil-sensitive component) was the total component of NMDA receptor responses subtracted with GluN2A component. GluN2A/B ratio was then calculated by dividing GluN2A component with GluN2B component.

Western blot analysis

Another set of adult male Wistar rats was divided into control and CSD group (n = 15, each group). Protocols for CSD stimulation using 3 mg of solid KCl for 45 minutes, combined with solid NaCl in control groups, were repeated.

After 45 minutes of SD stimulation by solid KCl, the isolated hippocampi were then homogenised in a solution containing RIPA buffer (lysis buffer; 150 mM NaCl, 20 mM Tris-HCl, 2 mM EDTA, 1 % Triton X-100, 0.05 % SDS, 1 mM PMSF, pH 8; Cell Signaling Technology,

Table 1 Comparison between CSD and Hippocampal SD Total number of spreading depression and amplitude were significantly reduced in the hippocampus compared to those in the cortex, while wave interval was significantly elevated in hippocampal SD. However, there was no significant changes in duration and AUC.

Parameters	CSD (n = 4)	Hippocampal SD (n = 4)	P-value
Total number of SD (waves /45 min)	9.23 ± 1.74	3.67 ± 0.58	0.004*
Amplitude (mV)	34.62 ± 6.78	24.79 ± 3.51	0.04*
Wave interval (min)	5.10 ± 1.49	10.53 ± 2.27	0.03*
Duration (s)	69.67 ± 19.60	74.14 ± 28.93	0.83
AUC (mV•s)	712.35 ± 187.77	810.46 ± 217.11	0.56

CSD and Hippocampal SD were elicited for 45 minutes using solid KCl. Glass electrodes were placed in both the neocortex (from bregma: anterior-posterior, +3 mm; lateral, 2 mm; and dorsal-ventral, 0.5 mm) and the ipsilateral hippocampus (from bregma: anterior-posterior, -4 mm; lateral, 2 mm). Data were analysed using the AcqKnowledge acquisition software. AUC, area under the curve; CSD, cortical spreading depression; SD, spreading depression; *P < 0.05 (independent sample two-tailed t-test).

Beverly, MA, USA) and Protease Inhibitor Cocktail (Cell Signaling Technology, Beverly, MA, USA). Tissue homogenates were centrifuged (Sigma-Aldrich, St. Louis, MO, USA) at 12,000 rpm; 4 ºC for 15 minutes.

Fifteen micrograms of protein were loaded onto a 7.5 % SDS-PAGE and electroblotted onto a polyvinylidene difluoride (PVDF) membrane (GE Healthcare Life Sciences, Little Chalfont, UK). Membranes that were intended to determine the quantity of GluN2A were blocked with 5 % bovine serum albumin (BSA) prior to incubation with the primary antibody in 5 % BSA at 4ºC overnight and incubated with horseradish peroxidase (HRP)-conjugated secondary antibody (1:10,000 dilution; anti-rabbit IgG antibody; Sigma-Aldrich, St. Louis, MO, USA) for 1 hour. For GluN2B detection, the membranes were blocked with 5 % TBST-MLK at room temperature for 1 hour and incubated with a primary antibody in 5 % TBST-MLK at 4 ºC overnight, and incubated with a HRP-conjugated secondary antibody (1:10,000 dilution; anti-mouse IgG antibody; Sigma-Aldrich, St. Louis, MO, USA) for 1 hour. The dilutions of the primary antibodies were 1:500 for both GluN2A (rabbit monoclonal antibody; Millipore, Billerica, MA, USA) and GluN2B (mouse monoclonal antibody; Millipore, Billerica, MA, USA) and 1:2,000 for β-actin (mouse monoclonal antibody; Sigma-Aldrich, St. Louis, MO, USA). Protein bands were sequentially detected using enhanced chemiluminescent (ECL) reagents (GE Healthcare Life Science, Little Chalfont, UK) exposed onto a hyperfilm (GE Healthcare Life Science, Little Chalfont, UK). The quantity of GluN2A and GluN2B were eventually measured using Image J software (NIH, Bethesda, MD, USA). These signals were normalised against β-actin bands.

Statistical analysis

All data were reported in the format of mean ± standard error of the mean (SEM). Statistical analysis was performed using IBM SPSS software version 20. Independent sample *t*-test was adopted in the analyses to establish a statistical correlation. Only probability values less than 0.05 ($P < 0.05$) were considered to be statistically significant.

Results

In vivo cortical and hippocampal DC recordings

Our data indicated that CSD propagated and reached the CA1 area of the hippocampus in an *in vivo* model with alteration of electrical properties. Several parameters characterising electrical properties of CSD and SD measured at the hippocampus (e.g. total number of SD
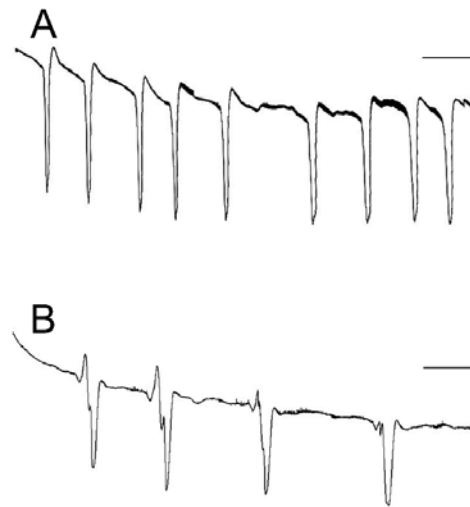

Fig. 1 Cortical and hippocampal DC recordings. (**A**) A representative tracing showing the DC shift in frontal cortex surface induced by KCl application (Scale bar: 5 min; 10 mV). (**B**) A representative tracing showing the DC shift in hippocampus induced by KCl application (Scale bar: 5 min; 10 mV). These tracings illustrated that SDs originated from the neocortex were shown to be able to spread to the hippocampus. The waves also appeared to be morphologically different between CSD and hippocampal SD. Recorded parameters were previously described in Table 1.

waves, amplitude, duration, AUC, and wave interval) are displayed in Table 1. In the cortical DC recording, the results showed that multiple shifts of negative DC characterised as SD were detected in the frontal neocortex in all rats ($n = 4$) which indicated that solid KCl application consistently induced multiple waves of CSD (Fig. 1A). In hippocampal DC recording, we illustrated that a series of negative DC potentials characterised as SD was detected in the hippocampal CA1 in all rats ($n = 4$; Fig. 1B).

Ratio of GluN2A/B response

Analysis of our current study revealed that GluN2A/B ratio of the CSD group significantly increased in comparison with the control group. After application of ifenprodil, NMDA receptor-mediated fEPSPs were reduced in both control and CSD slices (Fig. 2A). The reduced magnitudes of NMDA receptor-mediated fEPSPs in CSD and control slices were 23.5 ± 2.1 and 34.4 ± 5.5 %, respectively ($P = 0.092$; independent samples two-tailed *t*-test). However, the extent of this reduction was not significantly different between the CSD and control groups. In control slices, ifenprodil decreased NMDA receptor-mediated fEPSPs on the hippocampal CA1 by a degree comparable to other studies [17]. The GluN2A/B ratios in CSD and control groups were 3.376 ± 0.361 and 1.968 ± 0.346, respectively ($P = 0.018$; $n = 6$ each group; independent
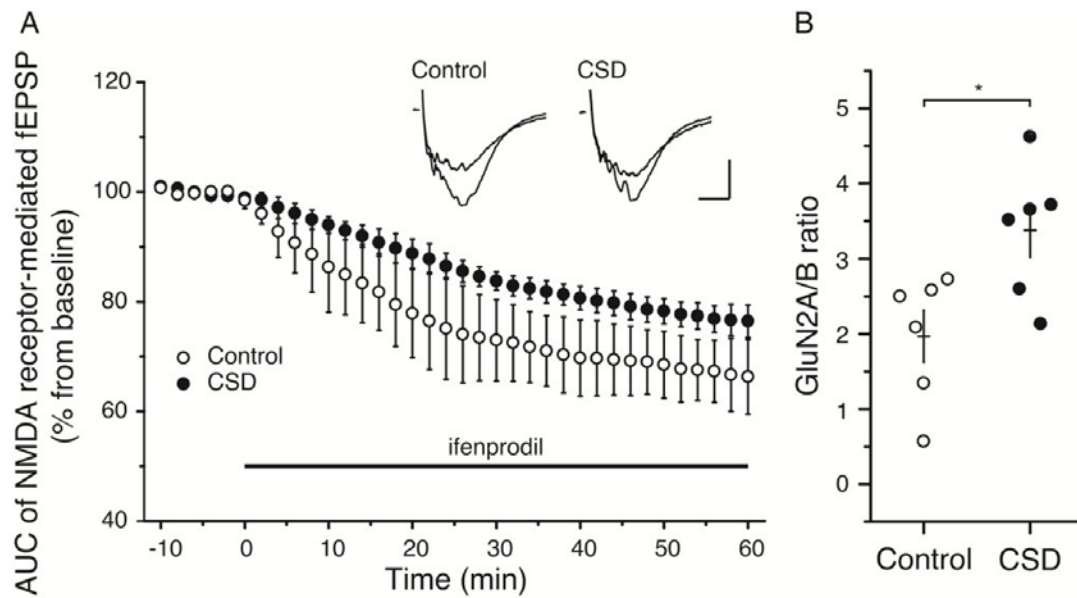
Fig. 2 CSD induction affected functional GluN2A/B ratio in hippocampal slices (**A**) Isolation of GluN2A component from NMDA receptor-mediated fEPSPs in the control and CSD groups. The reduction of NMDA receptor-mediated fEPSPs was stabilised within 40-60 minutes after ifenprodil application. GluN2A component was isolated by bath application of 3 μM ifenprodil, a GluN2B receptor antagonist, at time 0 to 60 min. Inset: Representative traces were recorded immediately prior to ifenprodil application and 60 minutes after ifenprodil application.

Calibration: 50 millisecond, 0.4 mV. The traces were normalised in terms of amplitude. (**B**) Data plot of the GluN2A/B ratio. The ratio of GluN2A/B was calculated by dividing the averaged AUC values of ifenprodil-insensitive component with those of ifenprodil-sensitive component at time 50 to 60 minutes. The GluN2A/B ratio was significantly elevated in hippocampal slices obtained from the CSD rats. $n = 6$ each group; $P < 0.05$ independent samples two-tailed t-test. Bar and whisker plots indicate the mean ± SEM.

samples two-tailed t-test; Fig. 2B). This result showed that CSD altered the responses of NMDA receptors in the hippocampal CA1 towards greater GluN2A/B response ratio. After treatment with ifenprodil, we also demonstrated that isolated fEPSPs were mediated by NMDA receptors, because the remaining fEPSPs were abolished by the NMDA receptor antagonist, APV (25 μM). Importantly, this GluN2A/B ratio represents the 'response' of GluN2A over GluN2B subunits on the neuronal plasma membrane.

Quantitative assay of GluN2A and GluN2B receptors

Our results obtained from Western blotting analysis showed that the total number of both ipsilateral GluN2A and GluN2B subunits of the NMDA receptor were significantly altered in CSD groups ($n = 15$; right KCl-placed hippocampus) compared to control groups ($n = 15$). We observed a significant increase in total number of GluN2A subunits and a reduction of those GluN2B subunits. The averaged intensity of GluN2A protein band relative to β-actin in ipsilateral CSD and control groups was 0.777 ± 0.040 and 0.655 ± 0.044, respectively ($P = 0.048$; independent samples two-tailed t-test). The averaged intensity of GluN2B protein band relative to β-

actin in ipsilateral CSD and control groups was 0.589 ± 0.027 and 0.713 ± 0.024, respectively ($P = 0.002$; independent samples two-tailed t-test; Fig. 3).

We also compared the total number of GluN2A and GluN2B subunits of the NMDA receptor between ipsilateral and contralateral sides of the hippocampus in CSD group. Total number of GluN2A subunits was significantly increased in the ipsilateral side of the hippocampus ($P = 0.042$; independent samples two-tailed t-test). The averaged values of protein intensity in both ipsilateral and contralateral side of the hippocampus were 0.777 ± 0.040 and 0.650 ± 0.047, respectively. In contrast, a significant reduction in the total number of GluN2B subunits was demonstrated with an averaged band intensity in both ipsilateral and contralateral side of 0.589 ± 0.027 and 0.699 ± 0.031, respectively ($P = 0.012$; independent samples two-tailed t-test). In addition, we compared a number of GluN2A and GluN2B subunits in contralateral CSD-induced hippocampi with those control hippocampi. These results were undoubtedly insignificant for both GluN2A and GluN2B subunits ($P = 0.826$ for GluN2A component; $P = 0.805$ for GluN2B component; independent samples two-tailed t-test).
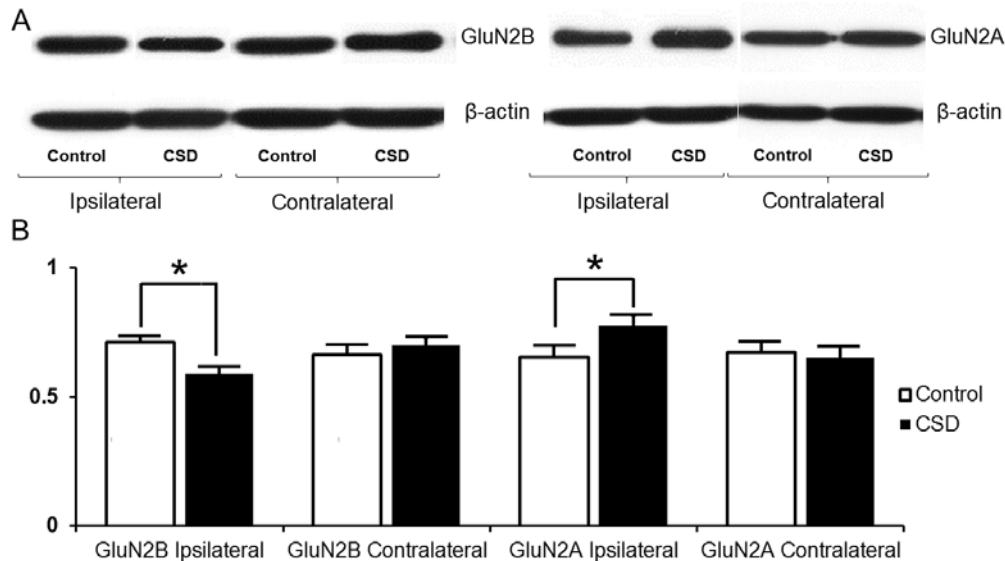
Fig. 3   Total number of GluN2A and GluN2B subunits of the NMDA receptor measured by Western blot analysis (**A**) The protein band intensities were exposed and normalised in association to the β-actin bands at 43 kDa. For both GluN2A and GluN2B, the signals derived from contralateral and ipsilateral hippocampi are depicted as well as those for CSD and control group. (**B**) Proportions of protein signal intensity over the β-actin were calculated and demographically presented in comparison with those of CSD and control groups. In CSD group, total number of GluN2A subunits of the NMDA receptor are significantly elevated while those of GluN2B are diminished. These findings are consistent with the result from our electrophysiological study towards greater GluN2A/B response ratio.

Discussion

Our study demonstrated that induction of CSD resulted in trains of DC shifting, compatible with hippocampal spreading depression. The results are consistent with previous *ex vivo* studies that CSD was induced by 2 M KCl microinjection [18, 19], or 3 mg solid KCl [9]. However, microinjection of 0.5 M KCl was shown not to produce DC shifting in the hippocampus [20]. Another study revealed that single CSD induced by 300 mM KCl topical application resulted in waves of SD in *in vivo* hippocampus only in FHM1 mutant mice, but not the wild-type mice [8]. These evidence support that propagation of SD from the neocortex into the hippocampus is increased in dose-dependent fashion.

According to the DC recordings, wave frequency and amplitude of hippocampal DC waves were diminished, while there were no significant changes in both duration and AUC. The duration of SD refers to how long ion channels remain open to enable prolongation of depolarisation. The AUC is the sum of the amplitude and duration. Wave frequency, which refers to the induction threshold, and amplitude were significantly diminished in hippocampal SD. Possible explanations may lie in anatomical difference [18, 21] and conduction sensitivity of the two structures.

Based on our electrophysiological studies, we observed an enhanced GluN2A/B ratio secondarily to CSD stimulation. Combining this information with our previous research [9], we pointed that LTP magnitude was significantly reduced in CSD group compared to the control group. These findings suggest that CSD may be able to alter hippocampal synaptic transmission by interfering GluN2A/B response ratio. Some evidence strongly suggest that ratio of GluN2A/B response governs bidirectional modification of LTP induction threshold in the CA1 of hippocampus [23, 24]. An increase in GluN2A/B ratio was shown to impair LTP, in which an increase of GluN2A/B ratio by one unit is associated with approximately 9 % reduction of LTP. [12, 25]

Findings from Western blotting analysis support our electrophysiological result of enhanced GluN2A/B ratio. We demonstrated that the total number of GluN2A subunits of the NMDA receptor was elevated whilst those of GluN2B were significantly diminished in the CSD group. Because CSD was elicited for only 45 minutes, we hypothesised that CSD causes post-translational modifications to GluN2A and GluN2B proteins rather than interfering with transcriptional processes. Although little is known regarding the precise mechanism by which GluN2A/B ratio alters the plasticity threshold, we propose that it involves the individual properties of both GluN2A and GluN2B subunits. Furthermore, we also showed that CSD may not travel to the contralateral hippocampus, because we observed no

significant changes of ipsilateral (right) and contralateral (left) in either the total number of individual GluN2A or GluN2B subunits.

Evidence from molecular experiments suggests that GluN2B receptors have longer activation duration than GluN2A, which results in a greater Ca^{2+} influx [26]; thus, overexpression of GluN2B led to the enhanced LTP in the hippocampus [27]. In addition, activation of GluN2B subunits of the NMDA receptor could generate LTP in GluN2A-knockout mice [23, 28] and hippocampal LTP was not observed in GluN2B-knockout mice [29].

Some limitations should be considered. First, since we used CSD as a model, the interpretation of our study may not only be constrained to migraine with aura, since various cerebral insults has been shown to produce CSD. Second, although the knowledge obtained from this study may explain hippocampus-associated symptoms during migraine aura, the behaviour or memory in animals were not evaluated. This, however, are being studied in our further research.

Taken together, our study revealed that CSD increased GluN2A/B ratio by modifying the numbers of GluN2A and GluN2B subtypes. Our previous studies [9] showed that repetitive CSD resulted in a reduction of LTP which, in turn, is correlated to impaired memory processes. Thus, it is suggested that increased GluN2A/B ratio is associated with reduced LTP. This physiological finding may be used to imply a temporal correlation between migraine with aura and hippocampus-associated symptoms. However, our study was conducted in animals, whether or not the possibility of our findings hold true in human remains unanswered.

References

1. Obrenovitch TP, Zilkha E (1995) High extracellular potassium, and not extracellular glutamate, is required for the propagation of spreading depression. J Neurophysiol 73:2107–2114.
2. Hadjikhani N, Sanchez del Rio M, Wu O, Schwartz D, Bakker D, Fischl B, Kwong KK, Cutrer FM, Rosen BR, Tootell RB, *et al* (2001) Mechanisms of migraine aura revealed by functional MRI in human visual cortex. Proc Natl Acad Sci USA 98:4687-4692.
3. Chen WT, Lin YY, Fuh JL, Hamalainen MS, Ko YC, Wang SJ (2011) Sustained visual cortex hyperexcitability in migraine with persistent visual aura. Brain 134:2387-2395.
4. Leao AAP (1944) Spreading depression of activity in the cerebral cortex. J Neurophysiol 7:359-390.
5. Crowell GF, Stump DA, Biller J, McHenry LC Jr, Toole JF (1984) The transient global amnesia-migraine connection. Arch Neurol 41(1):75-79.
6. Lin KH, Chen YT, Fuh JL, Li SY, Chen TJ, Tang CH, Wang SJ (2014) Migraine is associated with a higher risk of transient global amnesia: a nationwide cohort study. Eur J Neurol 21:718-724.
7. Olesen J, Jorgensen MB (1986) Leao's spreading depression in the hippocampus explains transient global amnesia. A hypothesis. Acta Neurol Scand 73:219-220.
8. Eikermann-Haerter K, Yuzawa I, Qin T, Wang Y, Baek K, Kim YR, Hoffmann U, Dilekoz E, Waeber C, Ferrari MD, van den Maagdenberg AMJM, Moskowitz MA, Ayata, C (2011) Enhanced Subcortical Spreading Depression in Familial Hemiplegic Migraine Type 1 Mutant Mice. J Neurosci 31(15): 5755–5763.
9. Maneepark M, Srikiatkhachorn A, Bongsebandhu-phubhakdi S (2012) Involvement of AMPA receptors in CSD-induced impairment of LTP in the hippocampus. Headache 52:1535-1545.
10. Laurie DJ, Bartke I, Schoepfer R, Naujoks K, Seeburg PH (1997) Regional, developmental and interspecies expression of the four NMDAR2 subunits, examined using monoclonal antibodies. Brain Res Mol Brain Res 51:23-32.
11. Philpot BD, Cho KK, Bear MF (2007) Obligatory role of NR2A for metaplasticity in visual cortex. Neuron 53:495-502.
12. Xu Z, Chen RQ, Gu QH, Yan JZ, Wang SH, Liu SY, Lu W (2009) Metaplastic regulation of long-term potentiation/long-term depression threshold by activity-dependent changes of NR2A/NR2B ratio. J Neurosci 29:8764-8773.
13. Kopp C, Longordo F, Nicholson JR, Luthi A (2011) Insufficient sleep reversibly alters bidirectional synaptic plasticity and NMDA receptor function. J Neurosci 26:12456-12465.
14. Kudo C, Toyama M, Boku A, Hanamoto H, Morimoto Y, Sugimura M, Niwa H (2013) Anesthetic effects on susceptibility to cortical spreading depression. Neuropharmacology 67:32-36.
15. Paxinos G, Watson C (2013) The rat brain in stereotaxic coordinates. 7th edition. Elsevier, Academic Press, New York, NY.
16. MacDougall MJ, Howland JG (2013) Acute stress and hippocampal output: exploring dorsal CA1 and subicular synaptic plasticity simultaneously in anesthetized rats. Physiol Rep 1(2):e00035.
17. Scimemi A, Fine A, Kullmann DM, Rusakov DA (2004) NR2B-containing receptors mediate cross talk among hippocampal synapses. J Neurosci 24:4767-4777.
18. Wernsmann B, Pape H, Speckmann E, Gorji A (2006) Effect of cortical spreading depression on synaptic transmission of rat hippocampal tissues. Eur J Neurosci 23:1103-1110.
19. Martens-Mantai T, Speckmann E, Gorji A (2014) Propagation of cortical spreading depression into the hippocampus: the role of the entorhinal cortex. Synapse 68:574-584.
20. Kunkler PE, Kraig RP (2003) Hippocampal spreading depression bilaterally activates the caudal trigeminal nucleus in rodents. Hippocampus 13:835-844.
21. De Curtis M, Pare D (2004) The rhinal cortices: A wall of inhibition between the neocortex and the hippocampus. Prog Neu-

robiol 74:101-110.

22. Pelletier JG, Apergis J, Pare D (2004) Low probability transmission of neocortical and entorhinal impulses through the perirhinal cortex. J Neurophysiol 91:2079-2089.

23. Weitlauf C, Honse Y, Auberson YP, Mishina M, Lovinger DM, Winder DG (2005) Activation of NR2A-Containing NMDA Receptors Is Not Obligatory for NMDA Receptor-Dependent Long-Term Potentiation. J Neurosci 25:8386-8390.

24. Philpot BD, Cho KK, Bear MF (2007) Obligatory role of NR2A for metaplasticity in visual cortex. Neuron 53:495-502.

25. Cui Z, Feng R, Jacobs S, Duan Y, Wang H, Cao X, Tsien JZ (2013) Increased NR2A:NR2B ratio compresses long-term depression range and constrains long-term memory. Sci Rep 3:1036.

26. Erreger K, Dravid SM, Banke TG, Wyllie DJA, Traynelis SF (2005) Subunit-specific gating controls rat NR1/NR2A and NR1/NR2B NMDA channel kinetics and synaptic signaling profiles. J Physiol 563.2:345-358.

27. Tang YP, Shimizu E, Dube GR, Rampon C, Kerchner GA, Zhuo M, Liu G, Tsien JZ (1999) Genetic enhancement of learning and memory in mice. Nature 401:63–69.

28. Kiyama Y, Manabe T, Sakimura K, Kawakami F, Mori H, Mishina M (1998) Increased thresholds for long-term potentiation and contextual learning in mice lacking the NMDA-type glutamate receptor epsilon1 subunit. J Neurosci 18:6704-6712.

29. Sprengel R, Suchanek B, Amico C, Brusa R, Burnashev N, Rozov A, Hvalby O, Jensen V, Paulsen O, Andersen P, *et al*. (1998) Importance of the intracellular domain of NR2 subunits for NMDA receptor fu nction in vivo. Cell 92:279-289.